Applied Mathematics & Information Sciences
An International Journal

Segmentation of Cerebral Edema Around Spontaneous Intracerebral Hemorrhage

Ming-Yang Chen[1,2], *Qing-Mao Hu*[1,2], *Zhen-Chuan Liu*[3], *Shou-Jun Zhou*[1,2] *and* **Xiao-Dong Li*[3]

[1] Shenzhen Institutes of Advanced Technology, Chinese Academy of Sciences, 1068 Xueyuan Boulevard, Shenzhen 518055, China
[2] Shenzhen Key Laboratory of Neuro-Psychiatric Modulation, Shenzhen, China
[3] Linyi People's hospital, 27 Eastern Section of The Jiefang Road, Liny, China

Received: 7 Jun. 2012; Revised 21 Sep. 2012; Accepted 23 Sep. 2012
Published online: 1 Mar. 2013

Abstract: An automatic method is presented to extract edema around spontaneous intracerebral hemorrhage (SICH). A new way to cluster edema based on region growing is proposed, with seeds derived from expectation-maximization algorithm, local grayscale mean derived from adaptive local thresholding with varied window sizes, and growing rules that combines local grayscale mean and grayscale information in the form of two-dimensional entropy. The algorithm has been validated on 36 patient datasets to achieve a Dice coefficient of 0.79 in less than 3 minutes. It may provide a potential tool for neurosurgeons to quantify edema and guide therapy of patients with SICH.

Keywords: Cerebral edema, spontaneous intracerebral hemorrhage, expectation maximization, local thresholding, region growing.

1. Introduction

Spontaneous intracranial hemorrhage (SICH) is one of the most common causes in adult acute neurologic injury, and it attracts much research attention for its high mortality and poor prognosis [1–3]. Cerebral edema is an important secondary brain injury after SICH. Major factors contributing to the death in acute stage of SICH caused by edema are intracranial hypertension and cerebral hernia [4]. Timely and effective diagnose and control of cerebral edema could help to reduce the mortality rate and prevent intracranial hypertension and cerebral hernia.

The mechanism of edema formation after SICH has not been fully understood [5]. Cerebral edema is present in most patients with SICH when imaged within 6h of onset, reaches the peak between 48h and 7 days, and is absorbed after 4 to 6 weeks [6].

Computed tomography (CT) head scans remain the first choice for diagnosing SICH. On head CT scans, it is difficult to delineate edema regions due to substantial overlap of grayscale ranges between the edema and other brain tissues (cerebrospinal fluid CSF and white matter WM) and unclear image boundaries. The major regions of cerebral edema candidates in patients with SICH are low grayscale regions around SICH within 1 centimeter radius of the normal brain tissues and the mirror areas on the other side [8]. Due to the importance to quantify edema, there have been some efforts on automatic or semi-automatic segmentation. Bardera et al. [7] proposed a semi-automated method based on level-set theory to achieve a matching ratio of 0.65. Bastian et al. [9] studied CT thresholds for edema to be 5-33 Hounsfield units (HU) using manually drawn hematoma from T2-weighted MRI. Sven et al. proposed a fuzzy expert system [10] and a hierarchical segmentation method [11] for edema segmentation. The last two studies did not report accuracy. The poor accuracy reflected the complexity and difficulty to segment edema. In this study, we propose an automatic algorithm to segment edema with better accuracy. It contains the following components: confining the edema within the neighborhood of hematoma, classifying edema by exploring the grayscale distribution of edema and neighboring tissues, and refining edema segmentation through combining local grayscale mean and local threshold by exploring local thresholding with adaptively varying window sizes. The algorithm has been tested against 36 patients with SICH to yield an average Dice coefficient of 79The rest are orga-

* Corresponding author: e-mail: lxd8199819@126.com

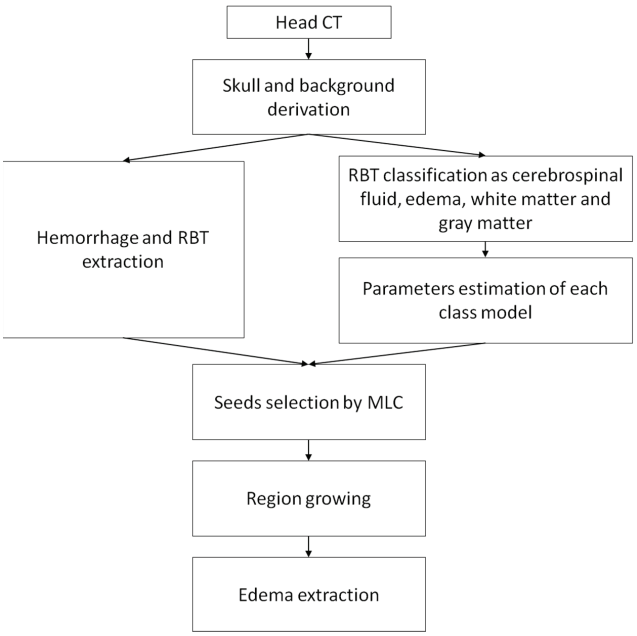

Figure 1: Block diagram of the segmentation process.

nized as follow. In section 2, the method and materials are presented. In section 3, the segmentation results are given and compared with manual segmentations. Discussion and conclusion are given at last.

2. Methods and Materials

There were 36 subjects from Linyi People's Hospital for this study. All the subjects were diagnosed with SICH and imaged within 6h to 72h. The statistics of the patients were: age range $[18,83]$ with an average 57 years, 13 female and 23 male. For each subject, an unenhanced head CT scan was performed. All the CT images were axial and obtained parallel to the orbito-meatal line. The image spacing is 0.46 mm within axial slices, and the slice distance is 4.8 mm. The manual segmentation was derived from three radiologists for validation. Fig. 1 shows the flowchart of the method. The proposed edema segmentation is accomplished in the following steps: 1) Preprocessing: Derive the brain and hematoma, and categorize the remaining brain tissues (RBT) as CSF, edema, WM and gray matter (GM) using k-means clustering. 2) Parameter estimation and automatic selection of seeds: Estimate the parameters of each normal distribution of the classified CSF, edema, WM and GM using expectation-maximization (EM), and select seeds using maximum likelihood clustering (MLC). 3) Region growing: Establish growing rules using local contrast and entropy information to find edema region. In the following subsections, details of the algorithm will be described.

2.1. Preprocessing

In a CT image, edema is the transition region between hematoma and normal tissue as shown in Fig. 2. Hematoma is extracted based on local thresholding [13], while the brain is derived from the head CT scan based on fuzzy C-means clustering and morphological process [12]. The RBT is first divided into dark and bright regions by local thresholding [13], then the dark regions and bright regions are further divided into initial CSF and edema, WM and GM by k-means clustering with two clusters as shown in Fig.3.

Consider the RBT in which $g(x,y) \in [0,255]$ is the grayscale of a pixel at location (x,y). In local adaptive threshold methods [13], the aim is to computed a threshold $thr(x,y)$ for each pixel such that

$$lable(x,y) = \begin{cases} 0, & g(x,y) > thr(x,y), \\ 255, & otherwise, \end{cases} \tag{1}$$

The threshold $thr(x,y)$ is computed using the grayscale mean $m(x,y)$ and standard deviation $s(x,y)$ in a window centered on the pixel(x,y):

$$thr(x,y) = m(x,y)[1+k(\frac{s(x,y)}{R}-1)] \tag{2}$$

where R is a constant, and k is a parameter which takes positive value in the range $[0.2,0.5]$. We enhance the original local thresholding scheme to calculate the loacl mean with varied window sizes such that the grayscale standard deviation reaches maximum.

2.2. Parameter estimation and seed selection

Grayscales of edema change with bleeding time. In our experimental data, edemas around hematoma generally have low density with unclear boundary. The grayscale rang of the manually drawn edema is from 12 to 50 HU, with an average and standard deviation of 29.3 and 5.9 HU, respectively. Through experiments we found that the histogram of edema accords well with normal distribution model. We compared three and four normal distributions to approximate the grayscale distribution of these four tissues respectively. Modeling the RBT by three normal distributions leads to disappearance of edema (Fig. 4(b)), while four normal distributions fit the original histogram well (Fig. 4(a)). Thus, the model adopted for RBT is a mixed Gaussian model of 4 normal distributions. The total probability density function of the mixture is given by

$$f(x,y) = \sum_{l=1}^{4} \omega_l f_l(x,y) \tag{3}$$

where l is the class number of the RBT, $f(x,y)$ is the grayscale value at pixel(x,y), and ω_l is the class proportion which sums to unity, $f_l(x,y)$ follows a normal distribution with mean μ_l and standard deviation σ_l.

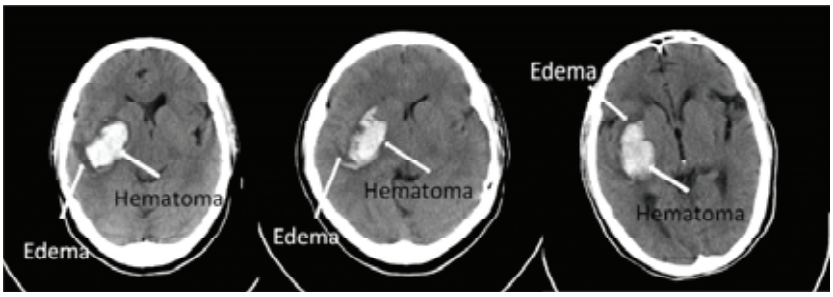

Figure 2: CT scans with edema surrounding the hematoma.

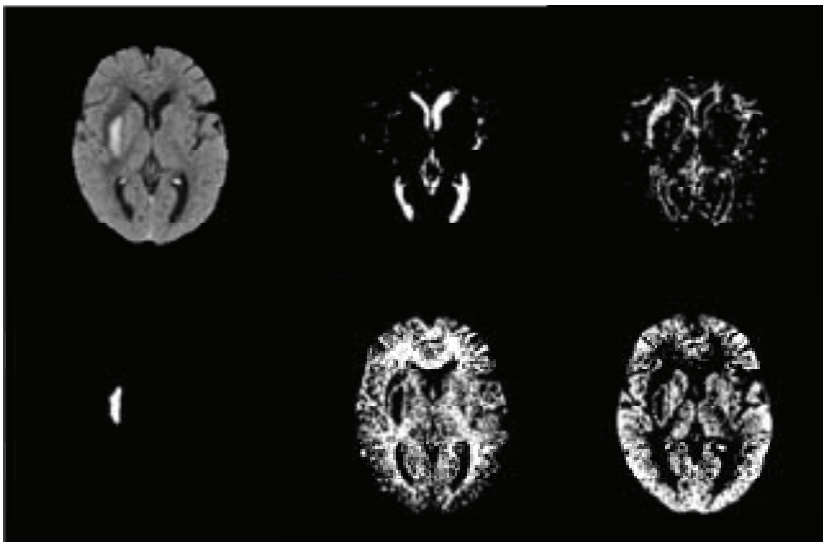

Figure 3: In the first row from left to right shows respectively, the extracted brain, initial regions of CSF, and edema; and the second row shows respectively, the hemorrhage region, the initial region of WM, and GM. Here k = 0.25, and R = 2.0xSdmax, where Sd_{max} is the maximum grayscale standard deviation of all pixels within the RBT

The parameters μ_l, σ_l, ω_l of each single normal distribution can be approximated and pixels of edema class can be classified by MLC. The class label of the edema class is denoted as G_2, while those of CSF, GM and WM are G_1, G_3 and G_4, respectively. We extract the edema seeds according to MLC. A pixel(x,y) belonging to the edema class should satisfy the following conditions:

–Its position should be near the hematoma.
–Its probability should be greater than the sum of other classes' probability

$$\omega_2 f_2(x_i,y_i) > \omega_l f_l(x_i,y_i), l = 1,3,4 \quad (4)$$

We estimate the 12 parameters using EM algorithm. The update equations are given by

$$\omega_l^{k+1} = \frac{1}{n}\sum_{i=0}^{I_{max}} h(i) f_l(G_l|i), l \in [1,4] \quad (5)$$

$$\mu_l^{k+1} = \frac{\sum_{i=0}^{I_{max}} h(i) f_l(G_l|i)}{\sum_{i=0}^{I_{max}} f_l(G_l|i)}, l \in [1,4] \quad (6)$$

$$(\sigma_l^2)^{k+1} = \frac{\sum_{i=0}^{I_{max}} (i-\mu_l^{k+1})^2 h(i) f_l(G_l|i)}{\sum_{i=0}^{I_{max}} f_l(G_l|i)}, l \in [1,4] \quad (7)$$

where N is the total number of pixels in the RBT, I_{max} the maximum grayscale in the RBT, $h(i)$ the frequency of grayscale i, and $f_l(G_l|i)$ the posteriori probability of the grayscale i that belongs to class G_l.

The first step is to calculate the initial parameters, which are set according to Table 1.

According to the Bayesian formulation, the posterior probability of the pixel(x,y) with true label l is given by

$$f(G_l|x,y) = \frac{\omega_l f_l(x,y)}{f(x,y)}, l \in [1,4] \quad (8)$$

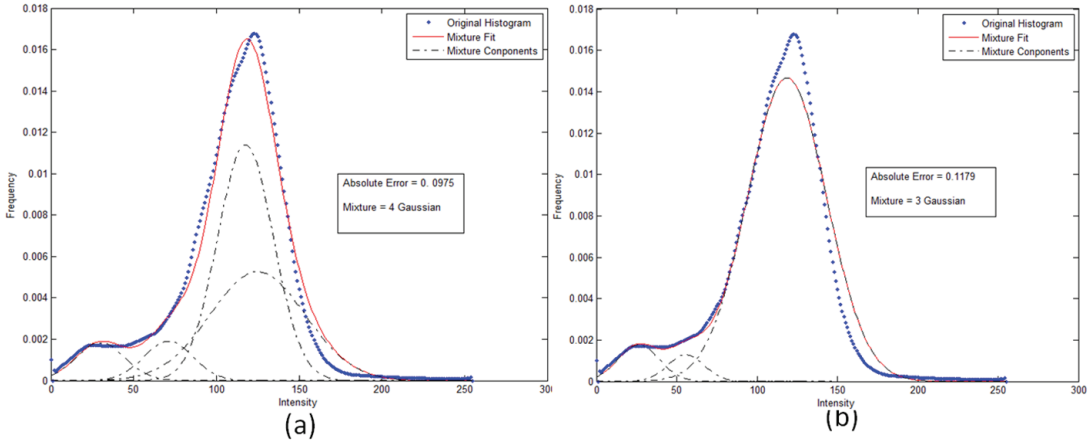

Figure 4: The left shows the RBT and the statistical model fitting result, The right shows edema and GM/WM and the model fitting result

Table 1: Initial values of the parameters are approximated through histogram analysis

Parameter	Value
$\mu_1^{init}/\mu_2^{init}/\mu_3^{init}/\mu_4^{init}$	grayscale mean of the initial class of CSF/edema/WM/GM
$(\sigma_1^2)^{init}/(\sigma_2^2)^{init}/(\sigma_3^2)^{init}/(\sigma_4^2)^{init}$	calculated using MLE from the samples of CSF/edema/WM/GM
$\omega_1^{init}/\omega_2^{init}/\omega_3^{init}/\omega_4^{init}$	proportion of initial CSF/edema/WM/GM in RBT

For a given pixel(x,y), the item $f(x,y)$ in Eq. (8) is invariant for each class. The Eq. (8) can be rewritten as

$$f(G_l|x,y) = \omega_l f_l(x,y), l \in [1,4] \tag{9}$$

The posterior probability is calculated by Eq. (9) and a pixel(x,y) is labeled according to maximized posterior probability.

2.3. Parameter estimation and seed selection

Image entropy reflects the average amount of information in the image. The one-dimensional (1D) entropy of image represents the grayscale clustering characteristics of image. Suppose P_i is the proportion of grayscale i, then the 1D entropy for an 8-bit image is given by

$$H = -\sum_{i=0}^{255} P_i ln P_i \tag{10}$$

As 1D entropy cannot reflect space information of grayscale distribution feature, a two-dimensional (2D) entropy to incorporate space information is proposed, which is composed of the grayscale and space characteristic of the grayscale distribution such as mean and variance.

We select grayscale mean value within the neighborhood of pixel(x,y) as the space characteristic of grayscale distribution. Then the mean value and pixel grayscale make up the characteristic pair(i,j), where i is the grayscale of pixel(x,y), and j represents the mean value within its neighborhood. The proportion of the characteristic pair and the 2D entropy are given by

$$P_{ij} = \frac{n(i,j)}{N^2} \tag{11}$$

$$H = -\sum_{i=0}^{255}\sum_{i=0}^{255} P_i ln P_i \tag{12}$$

where N is the number of pixels within RBT, $n(i,j)$ the occurrence frequency of pair(i,j).

Therefore, the rules of region growing are established as following:

- –The pixel grayscale value should be lower than the local threshold derived from local thresholding with adaptive window sizes;
- –The pixel grayscale probability should be greater than the sum of other classes' probability as shown in Eq. (4);
- –The 2D entropy of the pixel should be within the two peaks of 2D entropy histogram (Fig. 5). The peak 1 implies the pixels of the transit zone between edema and WM, while the peak 2 implies the pixels of the transit zone between edema and hematoma. The valley between the two peaks implies the pixels of the transit zone between edema and CSF.

Using these rules, the pixel can be classified as edema and other tissues.

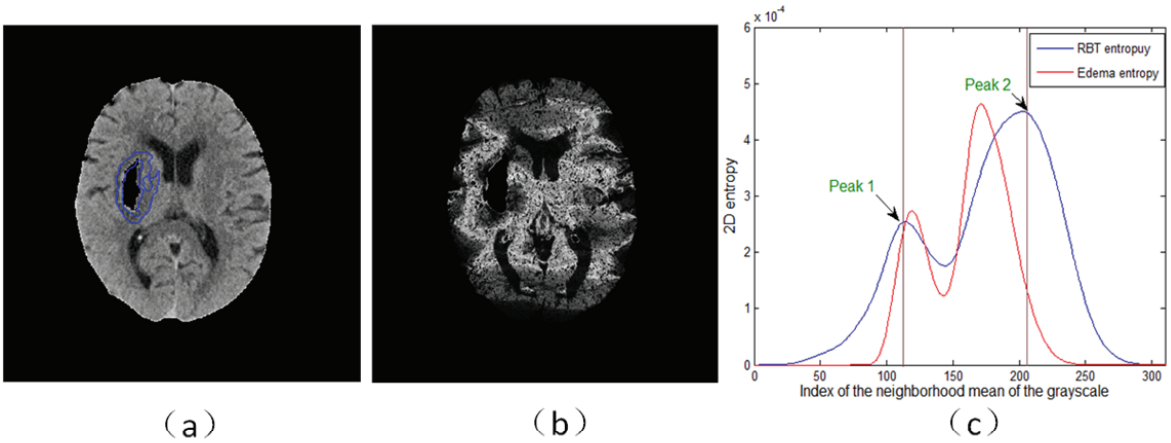

Figure 5: (a) the RBT image and edema boundary noted blue, (b) the 2D entropy of RBT shown as 8-bit image, (c) the 2D entropy shown in 2D axis

3. Result

The algorithm was tested on CT datasets of 36 patients. The visual comparison of the automatic method with the manual segmentation is shown in Fig. 6, where the ground truth (mannually drawn by 3 experts) is shown as the region within yellow boundaries on the original image.

False positive (FP), false negative (FN), matching ratio (Mr) and Dice coefficient ($Dice$) are used to quantify the performance of segmentation. They are calculated in the following way:

$$FP = \frac{Vol(A-G)}{Vol(G)} \tag{13}$$

$$FN = \frac{Vol(G-A)}{Vol(G)} \tag{14}$$

$$Mr = \frac{Vol(\cap GA)}{Vol(G)} \tag{15}$$

$$Dice = \frac{2*Vol(\cap GA)}{Vol(G)+Vol(A)} \tag{16}$$

where A and G represent the regions extracted by automatic method and ground truth respectively, $Vol(A)$ for the number of pixels within region A. The statistics of $Dice$, Mr, FP and FN for all tested datasets is given in Table 2.

4. Discussion and conclusion

4.1. Advantages

The image characteristic of cerebral edema may vary with time and/or seriousness of SICH. Cerebral edema can be divided into three levels according to water content clinically: mild cerebral edema, when CT value is 4-8 HU lower than the normal tissue; moderate cerebral edema, when CT value is 8-16 HU lower than the normal; severe cerebral edema, when CT value is more than 16 HU lower than the normal tissue.

The main challenge to segment cerebral edema is that the edema regions have unclear boundaries and have substantial grayscale overlap with other neighboring tissues. Compared with existing methods, the advantages of our method are listed below.

1) Automatic. A statistical model of RBT is established by using image preprocessing such as adaptive thresholding and K-means clustering, and the parameters of the model can be estimated automatically by EM algorithm. The seeds of cerebral edema region are found automatically. Region growing rules combines grayscale and spatial information without human intervention.

2) Adaptive. The local threshold and local grayscale mean are computed adaptively by changing the neighborhood window size to have maximum grayscale standard deviation. Then, the initial regions of CSF, edema, WM and GM are extracted and the 2D entropy of RBT is calculated. We used fixed window size 25x25 for comparison (Fig. 7). The $Dice$ coefficient, Mr, FP and FN are respectively 0.53, 0.49, 0.13 and 0.56 for the fixed window size algorithm, and 0.82, 0.80, 0.19 and 0.14 for the proposed method. We may thus argue that edema segmentation with adaptive window sizes is superior to that with fixed window size.

3) The neighborhood information constraint. The local mean value is used to calculate the 2D entropy, which is the main neighborhood information constrain in our method. For comparison, we carried out edema segmentation without neighborhood constrain to yield $Dice$ coefficient of 0.36, Mr of 0.81, FP of 2.24 and FN of 0.37, while these four metrics for our proposed method are respectively 0.83, 0.82, 0.06 and 0.12 for the case shown in Fig. 8. We may

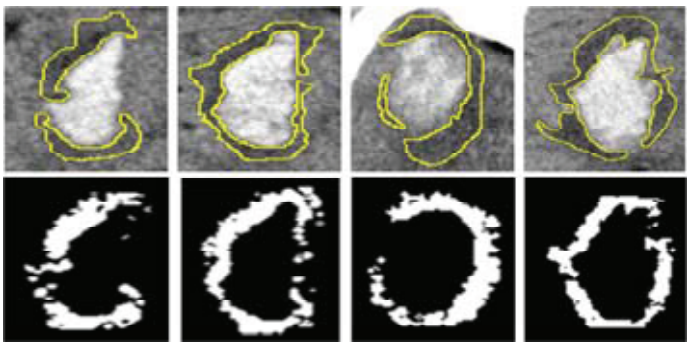

Figure 6: Comparative results of the automatic (white) and manual (regions within yellow boundaries) segmentation

Table 2: Statistics of the 36 tested datasets of the proposed algorithm

	Dice	*Mr*	*FP*	*FN*
Range	0.73-0.85	0.70-0.83	0.15-0.39	0.13-0.28
Mean	0.79	0.76	0.29	0.21
SD	0.03	0.04	0.13	0.04

Table 3: Statistics of the 36 tested datasets of thresholding range 5-33HU

	Dice	*Mr*	*FP*	*FN*
Range	0.19-0.76	0.46-0.96	0.10-7.08	0.01-0.55
Mean	0.54	0.80	1.83	0.20
SD	0.20	0.12	2.00	0.13

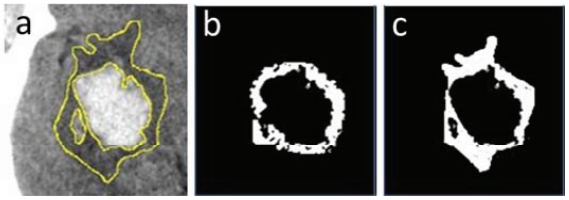

Figure 7: (a) the ground truth (region within yellow boundaries), (b) the results of the fixed window size method, (c) the result of our method

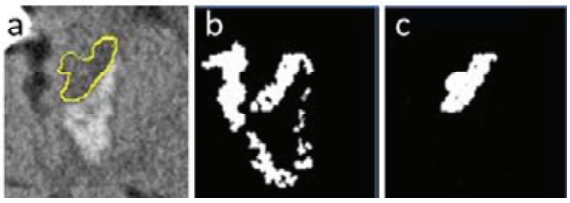

Figure 8: (a) the ground truth (region within yellow boundaries), (b) the results without neighborhood information constraint, (c) the result of our method

argue that the neighborhood information in the form of 2D entropy can enhance segmentation accuracy of edema.

4) Fast. The average time consumption of the method is 2 minutes and is distributed as follow: 1.31 minutes in preprocessing (mainly consumed on adaptive local thresholding, even though we have adopted integral images to speed up), 0.46 minutes in parameter estimation and seed calculation and 0.33 minutes in region growing. This average time is much shorter than existing methods to meet the real-time requirement for clinical use.

4.2. Sensitivity to parameters

Parameters k determine the initial class region. We change the k in [0.2, 0.5] to yield almost the same segmentation. Hence, the influence of their change on initialization can be compensated. Based on experiments we choose $k = 0.25$.

The algorithm is sensitive to the range of 2D entropy. The entropy of RBT has two peaks and the entropy of edema derived by radiologists is located between the two peaks (Fig. 5). The larger the range, the higher the value of FP; the smaller the range, the higher the value of FN. Choosing the range within the 2 peaks is a trade-off between FN and FP.

4.3. Comparison with existing methods

Existing methods except [7] did not provide quantification results. Our method achieved a better accuracy (average Mr of 0.76 vs 0.65) and shorter processing time (average 2 vs 4 minutes) than Bardera et al's method [7].

For comparison purpose, we carried out region growing with fixed threshold range 5-33HU according to [9]. *Dice* coefficient declined and FP rose up significantly (Table 3). We thus concluded that region growing with fixed

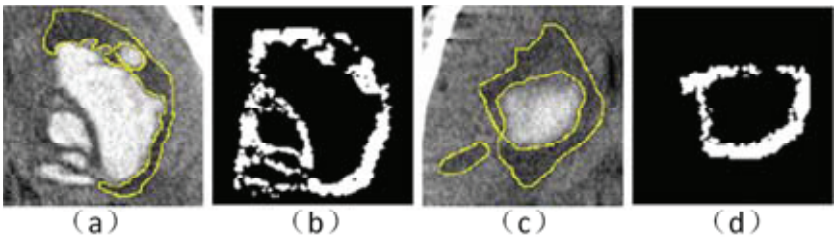

Figure 9: Cases with large segmentation errors

thresholds performed less well than the proposed algorithm.

4.4. Analysis of cases with large segmentation errors

There are two cases to be discussed for large errors. The first is the dataset with large hematoma (Fig. 9(a), (b)). Large hematoma will generally break into ventricles and make local contrasts higher than those of small hematoma, yielding a high FP. Fortunately these patients are generally suitable for surgery and less accurate edema quantification will not influence surgical indication.

The other one corresponds to subjects imaged after 48h, in which edema is in subacute or absorption period to have very unclear boundary (Fig. 9(c), (d)). This leads to a smaller edema regions with high FN. This problem is difficult to solve as the ground truth is not well defined.

From Fig. 9a, it can be seen serum pixels in between the two hematoma regions were misclassified by our algorithm as edema due to its similarity to edema in grayscales. This kind of segmentation error could be decreased by incorporation of anatomical knowledge.

4.5. Contributions and limitations

Our contributions are the following. First, we proposed to combine the spatial information to grow edema by introducing 2D entropy. Second, we proposed a way to adaptively calculate the local grayscale characteristics with varied window sizes.

The present study is not without limitations. Specifically, it cannot handle well cases when hematoma breaks into ventricles to have an area contact between edema and CSF. How to clearly define the boundary of edema and CSF becomes difficult even for medical experts. The algorithm performs less well when the hematoma is large or at subacute/absorption stage, where the contrasts may be high or low.

To conclude, we have proposed and validated an automatic algorithm to segment cerebral edema of patient with SICH through a new way to cluster edema based on region growing, with seeds derived from EM algorithm, local mean derived from adaptive local thresholding with varied window sizes, and growing rules that combine spatial (local mean) and grayscale information in the form of 2D entropy. This algorithm could provide a potential tool for neurosurgeons to quantify edema and guide therapy of patients with SICH.

Acknowledgement

This work is supported by: Key Joint Program of National Natural Science Foundation and Guangdong Province U1201257, One Hundred Talent Program of Chinese Academy of Sciences, Shenzhen Key Basic Research Project JC201005270370A, and introduced innovative R&D Teams of Guangdong Province ”Robot and Intelligent Information Technology” and ”Technologies for Image-guided Bio-simulation Radiotherapy Machinery”.

References

[1] Joseph, P.B., Harold P.A., William, B., William, F., Edward, F., James, G., Carlos, K., Derek, K., Marc, M., Barbara, T., Joseph, M.Z., Mario, Z.. Guidelines for the management of spontaneous intracerebral hemorrhage. Stroke,**30**, 905-915 (1999).

[2] Joseph, P.B., Thomas, B., Rosemary, M., Gertrude, H.. Intracerebral hemorrhage more than twice as common as subarachnoid hemorrhage. Journal of Neurosurgery,**78**, 188-191 (1993).

[3] Caplan, L.R.. Intracerebral hemorrhage. Lancet,**339**, 656-658 (1992).

[4] Broderick, J.P., Brott, T.G., Duldner, J.E., Tomsick, T., Huster, G.. Volume of intracerebral hemorrhage. A powerful and easy-to-use predictor of 30-day mortality. Stroke,**24**, 987-993 (1993).

[5] Xi,G., Hua, Y., Bhasin, R.R., Ennis, S.R., Keep, R.F., Hoff, J.T.. Mechanisms of edema formation after intracerebral hemorrhage: effects of extravasated red blood cells on blood flow and blood-brain barrier integrity. Stroke,**32**, 2932-2938 (2001).

[6] David, Z., Wang, D.O., Arun, V., Talkad, M.D.. Treatment of intracerebral hemorrhage: what should we do now? Current Neurology and Neuroscience Report,**9**, 13-18 (2009).

[7] Bardera, A., Boada, I., Feixas, M., Remollo, S., Blasco, G., Silva, G., Pedraza, S.. Semi-automated method for brain hematoma and edema quantification using computed tomography. Computerized Medical Imaging and Graphics,**33**, 304-311 (2009).
[8] Enrico, F., Massimo, B., Andrea, S., Roberta, S., Cristiano., Michele, C., Stefano, C., Riccardo, T., Arturo, C.. CT perfusion mapping of hemodynamic disturbances associated to acute spontaneous intracerebral hemorrhage. Neuroradiology,**50**, 729-740 (2008).
[9] Bastian, V., Dimitre, S., Ingrid, W., Arnd, D., Marc, S., Stefan, S., Jurgen, B.. Semi-automatic volumetric assessment of perihemorrhagic edema with computed tomography. European Journal of Neurology. Doi,**10**, 1111/j, 1468-1331, 03395x (2011).
[10] Sven, L., Domagoj, L., Dubravko, C.. Fuzzy expert system for edema segmentation. In: 9th Electrotechnical Conference on Mediterranean,**2**, 1476-1479 (1998).
[11] Sven, L., Dubravko, C., Atam, P.D.. Hierarchical segmentation of CT head images. In: 18th Annual International Conference of the IEEE Engineering in Medicine and Biology Society. MR-CT Brain Image Analysis. 736-737, IEEE Press, Amsterdam (1996).
[12] Hu,Q., Qian, G., Aziz, A., Nowinski, W.L.. Segmentation of brain from computed tomography head images. In: 27th Annual Conference of the Engineering in Medicine and Biology Society, pp 3375-3378 (2005).
[13] Sauvola, J., Pietikainen, M.. Adaptive document image binarization. Pattern Recognition,**33**, 225-236 (2000).

Ming-Yang Chen is a doctoral student at Shenzhen Institutes of Advanced Technology, Chinese Academy of Sciences, China. His current research interests include image analysis, computer-aided diagnoses and therapy, and pattern recognition.

Qing-Mao Hu (technical correspondence author) is a professor, director of Laboratory for Medical Imaging and Digital Surgery at Shenzhen Institutes of Advanced Technology, Chinese Academy of Sciences, China. He obtained his PhD from Huazhong University of Science and Technology in 1990. He proposed the image segmentation framework by combining prior knowledge in the form of background proportion, constraints on contrast and transition regions, with traditional image processing methods. He led a team to have developed robust image analysis systems for both hemorrhage and ischemic strokes that have been used in national hospitals and international cooperation. He has published more than 100 papers and filed more than 20 international inventive patents. His research areas include: neural image analysis, robust medical image processing, computer-aided diagnosis and therapy, computer vision, and pattern recognition.

Xiao-Dong Li (clinical correspondence author) is a consultant radiologist of general radiology and is presently director of Medical Imaging Department of Linyi People's Hospital affiliated to Shandong University. He is an active researcher with 27 years experience of medical imaging diagnosis of general radiology and image-guided interventional radiology. He has published more than 20 papers on medical imaging and interventional radiology.